

Nonlinear oscillatory convective regimes in a three-layer system with an inclined temperature gradient

Ilya B. Simanovskii

Department of Mathematics, Technion–Israel Institute of Technology, 32000 Haifa, Israel

(Received 26 January 2011; revised manuscript received 18 May 2011; published 14 July 2011)

The influence of the horizontal component of the temperature gradient on nonlinear regimes of oscillatory convection developed under the joint action of buoyant and thermocapillary effects in a multilayer system is investigated. Two-dimensional convective regimes are studied by the finite difference method. Rigid heat-insulated lateral walls are considered. It is found that the region of nonlinear asymmetric oscillations is restricted by the Grashof number values, both from below and from above, by the steady states.

DOI: [10.1103/PhysRevE.84.016306](https://doi.org/10.1103/PhysRevE.84.016306)

PACS number(s): 47.55.pf

I. INTRODUCTION

Convective phenomena in fluid systems with an interface have been the subject of an extensive investigation over the past few decades. Several classes of instabilities have been found (for a review, see Refs. [1] and [2]).

There are two basic physical phenomena that produce convective instability in systems with an interface: buoyancy and the thermocapillary effect. When heating is from below, buoyancy instability generates the Rayleigh–Bénard convection [3], while the thermocapillary effect is the origin of the Marangoni–Bénard convection [1,4]. The case where both effects act simultaneously is the most typical.

One of the interesting phenomena caused by the joint action of buoyancy and the thermocapillary effect is the appearance of oscillatory instability of the mechanical equilibrium upon heating from below. This phenomenon was first discovered in the case of a two-layer system [1,5,6]. A similar phenomenon under the joint action of both mechanisms of instability in a multilayer system has been studied for *free heat-insulated lateral walls* in [7] and in the case of *periodic boundary conditions on lateral boundaries* in [8] and [9]. Specifically, in [8] and [9] it was found that the competition of both mechanisms of instability could lead to the development of nonlinear buoyant-thermocapillary traveling waves and modulated traveling waves.

In reality, it is difficult to guarantee that the temperature gradient is directed strictly perpendicularly to the interfaces. Under experimental conditions, the temperature gradient is not perfectly vertical and the horizontal component of the temperature gradient appears. The appearance of this component changes the situation completely: at any small values of the Marangoni number ($M \neq 0$), the mechanical equilibrium becomes impossible, and a convective flow takes place in the system. Thus, it is reasonable to consider the influence of the horizontal component of the temperature gradient on convective regimes developed in the system.

The Marangoni convection with the inclined temperature gradient in the “symmetric” multilayer system, when the exterior layers have the same thermophysical properties, has been investigated in [10].

The interaction of buoyant and thermocapillary mechanisms of instability under the action of the inclined temperature gradient in *multilayer systems* has not been studied to our knowledge.

In the present paper, the influence of the horizontal component of the temperature gradient on nonlinear oscillatory convective regimes, developed under the joint action of buoyant and thermocapillary effects in the system air–ethylene glycol–fluorinert FC75, is studied. Transitions between convective flows with different spatial structures are investigated.

The paper is organized as follows. In Sec. II, the mathematical formulation of the problem in a three-layer system is presented. The nonlinear approach is described in Sec. III. Nonlinear simulations of the finite-amplitude convective regimes are considered in Sec. IV. Section V contains some concluding remarks.

II. GENERAL EQUATIONS AND BOUNDARY CONDITIONS

Let the space between two rigid horizontal plates be filled by three immiscible viscous fluids with different physical properties (see Fig. 1). The equilibrium thickness of each layer is a . We assume that the deformations of interfaces are small, and their influence on the flow and temperature distribution can be ignored. The m th fluid has density ρ_m , kinematic viscosity ν_m , dynamic viscosity $\eta_m = \rho_m \nu_m$, thermal diffusivity χ_m , heat conductivity κ_m and heat expansion coefficient β_m . The surface tension coefficients on the upper and lower interfaces, σ and σ_* , are linear functions of temperature T : $\sigma = \sigma_0 - \alpha T$, $\sigma_* = \sigma_{*0} - \alpha_* T$. The acceleration due to gravity is g . The temperature on the horizontal plates $z = a_1$ and $z = -a_2 - a_3$ is fixed in the following way: $T(x, z, a_1) = -A_h x + \theta$, $T(x, z, -a_2 - a_3) = -A_h x$, $A_h > 0$. The vertical lateral boundaries $x = 0$ and $x = l$ are heat-insulated.

We define

$$\begin{aligned} \rho &= \frac{\rho_1}{\rho_2}, & \nu &= \frac{\nu_1}{\nu_2}, & \eta &= \frac{\eta_1}{\eta_2} = \rho \nu, \\ \chi &= \frac{\chi_1}{\chi_2}, & \kappa &= \frac{\kappa_1}{\kappa_2}, & \beta &= \frac{\beta_1}{\beta_2}, \\ a &= \frac{a_2}{a_1}, & \rho_* &= \frac{\rho_1}{\rho_3}, & \nu_* &= \frac{\nu_1}{\nu_3}, \\ \eta_* &= \frac{\eta_1}{\eta_3} = \rho_* \nu_*, & \chi_* &= \frac{\chi_1}{\chi_3}, & \kappa_* &= \frac{\kappa_1}{\kappa_3}, \\ \beta_* &= \frac{\beta_1}{\beta_3}, & a_* &= \frac{a_3}{a_1}, & \bar{\alpha} &= \frac{\alpha_*}{\alpha}. \end{aligned}$$

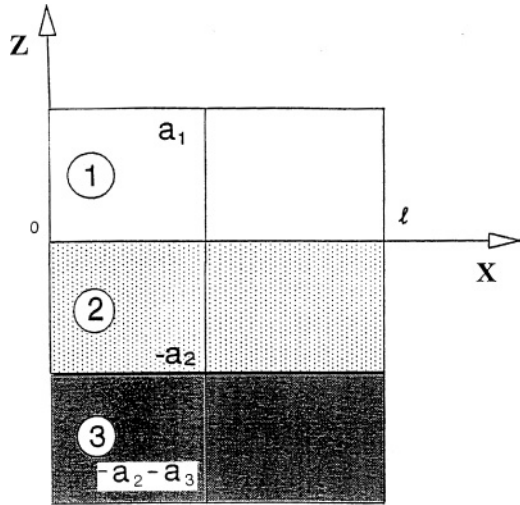


FIG. 1. Geometrical configuration of the three-layer system and coordinate axes.

As the units of length, time, velocity, pressure, and temperature, we use a_1 , a_1^2/v_1 , v_1/a_1 , $\rho_1 v_1^2/a_1^2$, and θ . The complete nonlinear equations governing convection are then written in the following dimensionless form:

$$\frac{\partial \mathbf{v}_m}{\partial t} + (\mathbf{v}_m \cdot \nabla) \mathbf{v}_m = -e_m \nabla p_m + c_m \Delta \mathbf{v}_m + b_m G T_m \mathbf{e}, \quad (1)$$

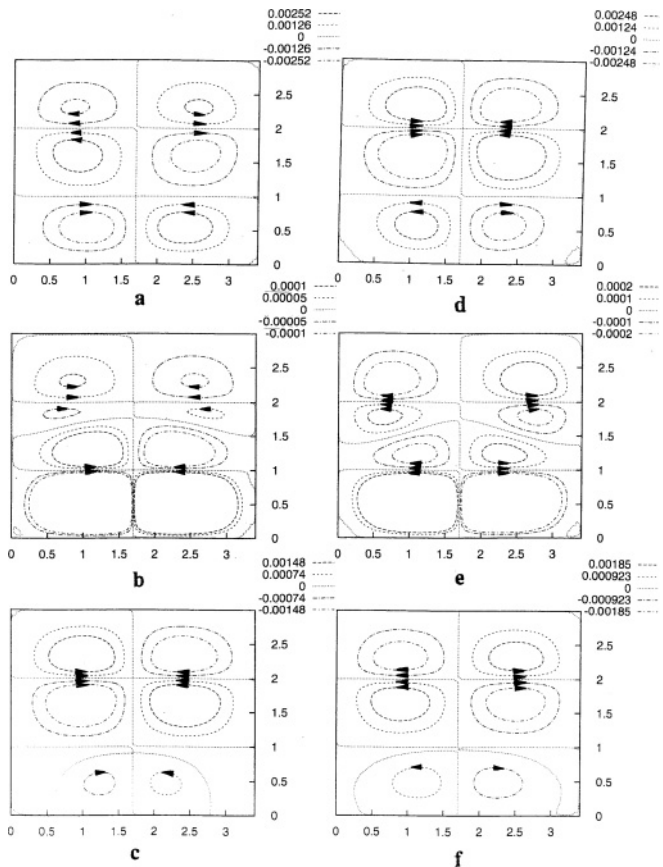


FIG. 2. A time sequence of snapshots of streamlines for the symmetric time-periodic motion at $\epsilon = 0$, $G = 2.15$, $K = 3682$, and $L = 3.4$.

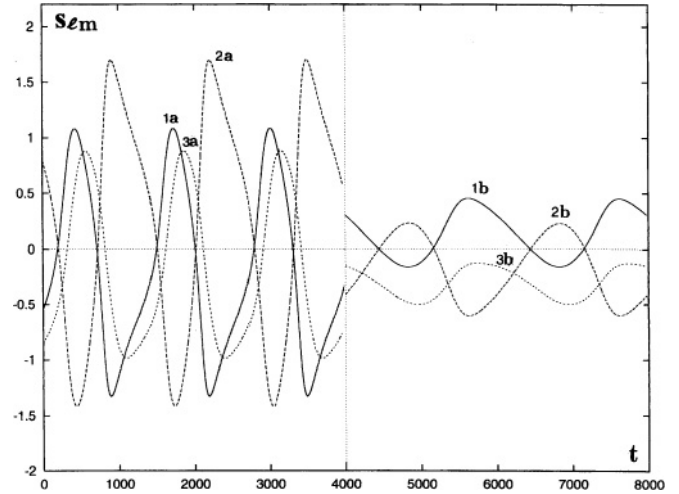


FIG. 3. Dependencies of $S_{l,m}$ on time ($m = 1, 2, 3$) at $\epsilon = 0$ (lines 1a, 2a, 3a) and $\epsilon = 0.01$ (lines 1b, 2b, 3b); $G = 2.15$, $K = 3682$.

$$\frac{\partial T_m}{\partial t} + \mathbf{v}_m \cdot \nabla T_m = \frac{d_m}{P} \Delta T_m, \quad (2)$$

$$\nabla \cdot \mathbf{v}_m = 0, \quad m = 1, 2, 3, \quad (3)$$

where $e_1 = c_1 = b_1 = d_1 = 1$, $e_2 = \rho$, $c_2 = 1/v$, $b_2 = 1/\beta$, $d_2 = 1/\chi$, $e_3 = \rho_*$, $c_3 = 1/v_*$, $b_3 = 1/\beta_*$, and $d_3 = 1/\chi_*$; $\Delta = \nabla^2$, $G = g\beta_1\theta a_1^3/v_1^2$ is the Grashof number, and $P = v_1/\chi_1$ is the Prandtl number determined by the parameters of the top layer; and \mathbf{e} is the unit vector of the axis z .

The conditions on the rigid horizontal boundaries are as follows.

$$z = 1: \quad v_1 = 0, \quad T_1 = -\epsilon x \quad (4)$$

$$z = -2: \quad v_3 = 0, \quad T_3 = -\epsilon x + 1. \quad (5)$$

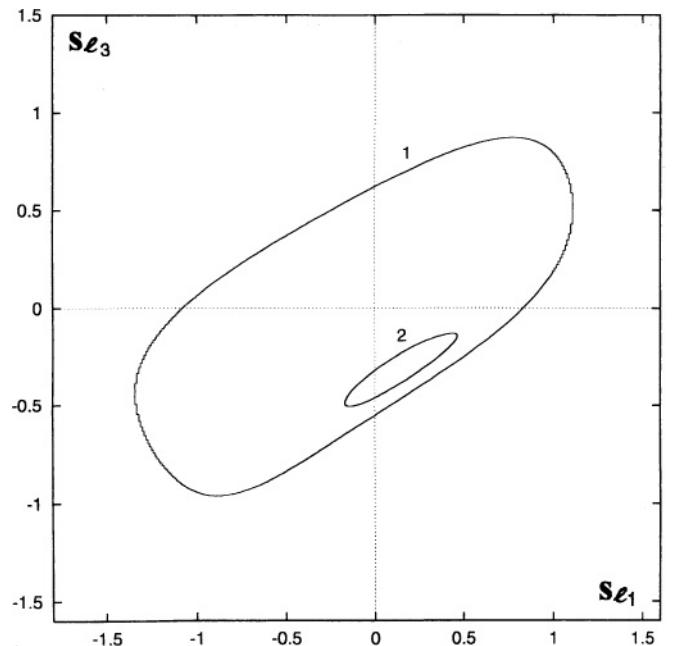


FIG. 4. Phase trajectory in the plane (S_{l1}, S_{l3}) for oscillatory motion at $\epsilon = 0$ (line 1) and $\epsilon = 0.01$ (line 2); $G = 2.15$; $K = 3682$.

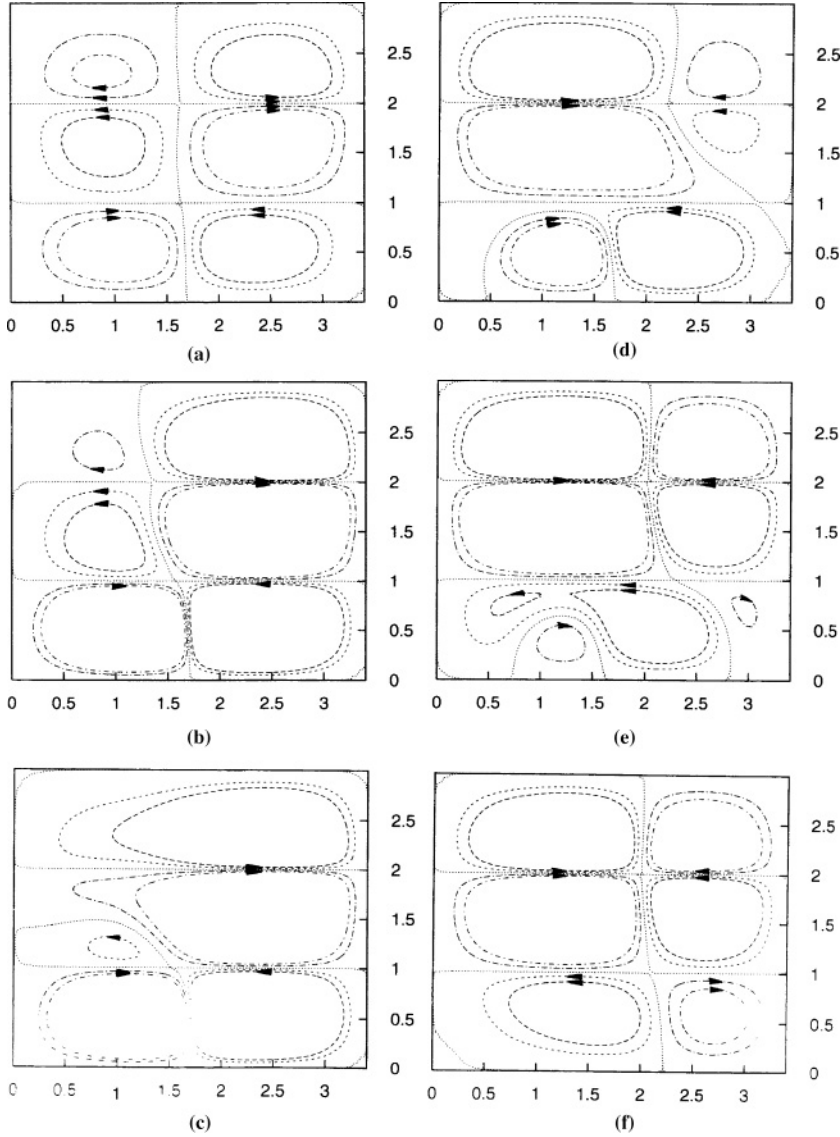


FIG. 5. Time sequence of snapshots of streamlines for the asymmetric time-periodic motion during one period at $\epsilon = 0.00082$, $G = 2.15$, and $K = 3682$.

Here $\epsilon = A_h a_1 / \theta > 0$ is the nondimensional parameter characterizing the horizontal component of the temperature gradient. The boundary conditions on the interface $z = 0$ can be written in the form

$$\begin{aligned} \eta \frac{\partial v_{1x}}{\partial z} - \frac{\partial v_{2x}}{\partial z} - \frac{\eta M}{P} \frac{\partial T_1}{\partial x} &= 0, \\ \eta \frac{\partial v_{1y}}{\partial z} - \frac{\partial v_{2y}}{\partial z} - \frac{\eta M}{P} \frac{\partial T_1}{\partial y} &= 0, \end{aligned} \quad (6)$$

$$v_{1x} = v_{2x}, \quad v_{1y} = v_{2y}, \quad v_{1z} = v_{2z}, \quad (7)$$

$$T_1 = T_2, \quad (8)$$

$$\kappa \frac{\partial T_1}{\partial z} = \frac{\partial T_2}{\partial z} \quad (9)$$

and at $z = -1$,

$$\begin{aligned} \eta^{-1} \frac{\partial v_{2x}}{\partial z} - \frac{\partial v_{3x}}{\partial z} - \frac{M}{P} \frac{\partial T_2}{\partial x} &= 0, \\ \eta^{-1} \frac{\partial v_{2y}}{\partial z} - \frac{\partial v_{3y}}{\partial z} - \frac{M}{P} \frac{\partial T_2}{\partial y} &= 0, \end{aligned} \quad (10)$$

$$v_{2x} = v_{3x}, \quad v_{2y} = v_{3y}, \quad v_{2z} = v_{3z}, \quad (11)$$

$$T_2 = T_3, \quad (12)$$

$$\kappa^{-1} \frac{\partial T_2}{\partial z} = \frac{\partial T_3}{\partial z}. \quad (13)$$

Here $P = \nu_1 / \chi_1$ is the Prandtl number for the liquid in layer 1 and $M = \alpha \theta a / \eta_1 \chi_1$ is the Marangoni number.

The conditions on the solid lateral boundaries, which are assumed to be thermally insulated, are as follows.

$$x = 0, L: \quad v_m = 0, \quad \frac{\partial T_m}{\partial x} = 0, \quad m = 1, 2, 3. \quad (14)$$

The above-mentioned boundary value problem in the case $\epsilon = 0$ has the solution

$$v_m = 0, \quad p_m = 0, \quad m = 1, 2, 3, \quad (15)$$

$$T_1 = T_1^0 = -\frac{(z-1)}{2+\kappa}, \quad (16)$$

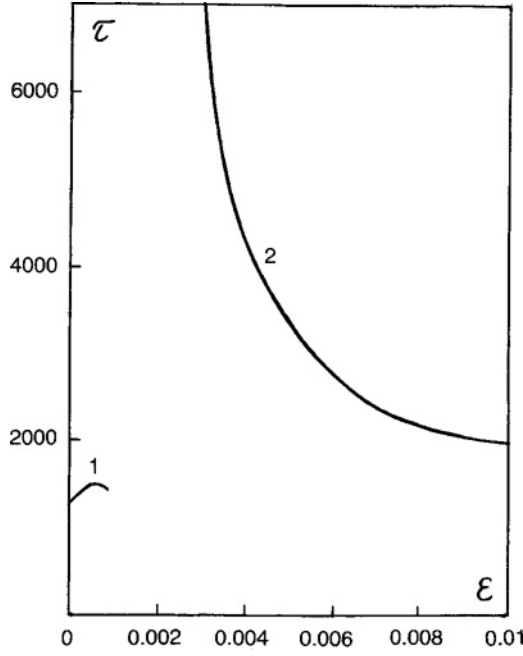


FIG. 6. Dependence of the period of oscillations on ϵ . $G = 2.15$; $K = 3682$.

$$T_2 = T_2^0 = -\frac{(\kappa z - 1)}{2 + \kappa}, \quad (17)$$

$$T_3 = T_3^0 = -\frac{(z - 1) + (1 - \kappa)}{2 + \kappa}, \quad (18)$$

corresponding to the mechanical equilibrium state. Depending on the physical parameters of fluids, the mechanical equilibrium state may become unstable with respect to different instability modes. In the case $\epsilon \neq 0$, mechanical equilibrium is impossible, in principle, and convective motion appears in the system.

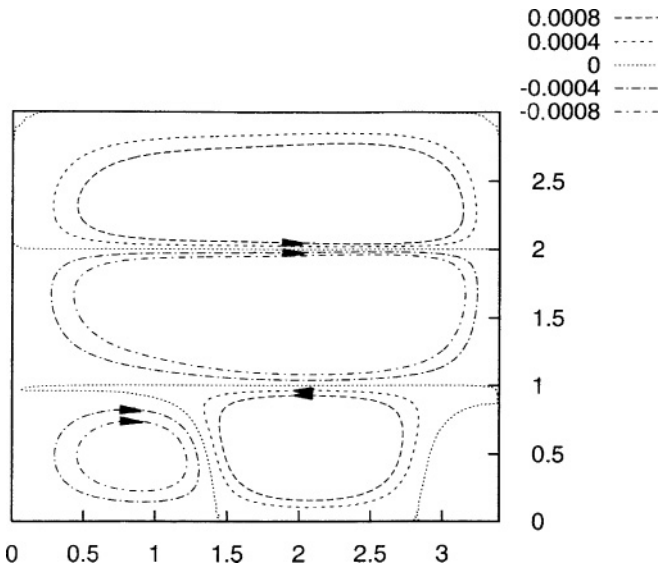


FIG. 7. Streamlines for the asymmetric steady state at $\epsilon = 0.00092$, $G = 2.15$, and $K = 3682$.

III. NONLINEAR APPROACH

To investigate the flow regimes generated by the convective instabilities, we perform nonlinear simulations of two-dimensional flows [$v_{my} = 0$ ($m = 1, 2, 3$); the fields of physical variables do not depend on y]. In this case, we can introduce the stream function ψ_m and the vorticity ϕ_m ,

$$v_{m,x} = \frac{\partial \psi_m}{\partial z}, \quad v_{m,z} = -\frac{\partial \psi_m}{\partial x},$$

$$\phi_m = \frac{\partial v_{m,z}}{\partial x} - \frac{\partial v_{m,x}}{\partial z} \quad (m = 1, 2, 3),$$

and rewrite Eqs. (1)–(3) in the following form:

$$\frac{\partial \phi_m}{\partial t} + \frac{\partial \psi_m}{\partial z} \frac{\partial \phi_m}{\partial x} - \frac{\partial \psi_m}{\partial x} \frac{\partial \phi_m}{\partial z} = d_m \Delta \phi_m + b_m G \frac{\partial T_m}{\partial x}, \quad (19)$$

$$\Delta \psi_m = -\phi_m, \quad (20)$$

$$\frac{\partial T_m}{\partial t} + \frac{\partial \psi_m}{\partial z} \frac{\partial T_m}{\partial x} - \frac{\partial \psi_m}{\partial x} \frac{\partial T_m}{\partial z} = \frac{c_m}{P} \Delta T_m \quad (m = 1, 2, 3). \quad (21)$$

At the interfaces normal components of velocity vanish and the continuity conditions for tangential components of velocity, viscous stresses, temperatures, and heat fluxes also apply.

$$z = 0: \quad \psi_1 = \psi_2 = 0, \quad \frac{\partial \psi_1}{\partial z} = \frac{\partial \psi_2}{\partial z}, \quad T_1 = T_2, \quad (22)$$

$$\frac{\partial T_1}{\partial z} = \frac{1}{\kappa} \frac{\partial T_2}{\partial z}, \quad \frac{\partial^2 \psi_1}{\partial z^2} = \frac{1}{\eta} \frac{\partial^2 \psi_2}{\partial z^2} + \frac{M}{P} \frac{\partial T_1}{\partial x}. \quad (23)$$

$$z = -a: \quad \psi_2 = \psi_3 = 0, \quad \frac{\partial \psi_2}{\partial z} = \frac{\partial \psi_3}{\partial z}, \quad T_2 = T_3, \quad (24)$$

$$\frac{1}{\kappa} \frac{\partial T_2}{\partial z} = \frac{1}{\kappa_*} \frac{\partial T_3}{\partial z}, \quad \frac{1}{\eta} \frac{\partial^2 \psi_2}{\partial z^2} = \frac{1}{\eta_*} \frac{\partial^2 \psi_3}{\partial z^2} + \frac{\bar{\alpha} M}{P} \frac{\partial T_2}{\partial x}. \quad (25)$$

On horizontal solid plates,

$$z = 1: \quad \psi_1 = \frac{\partial \psi_1}{\partial z} = 0, \quad T_1 = -\epsilon x; \quad (26)$$

$$z = -2: \quad \psi_3 = \frac{\partial \psi_3}{\partial z} = 0, \quad T_3 = -\epsilon x + 1. \quad (27)$$

On solid heat-insulated lateral walls,

$$x = 0, L: \quad \psi_m = \frac{\partial \psi_m}{\partial x} = \frac{\partial T_m}{\partial x} = 0 \quad (m = 1, 2, 3). \quad (28)$$

The boundary value problem formulated above was solved by the finite-difference method. Equations were approximated on a uniform mesh using a second-order approximation for the spatial coordinates. Nonlinear equations were solved using an explicit scheme, on a rectangular uniform mesh, 56×112 . We checked the results on 56×168 and 112×168 meshes. The relative changes of the stream function amplitudes for all the mesh sizes do not exceed 2.5%. The time step was calculated by the formula

$$\Delta t = \frac{[\min(\Delta x, \Delta z)]^2 [\min(1, \nu, \chi, \nu_*, \chi_*)]}{2[2 + \max|\psi_m(x, z)]},$$

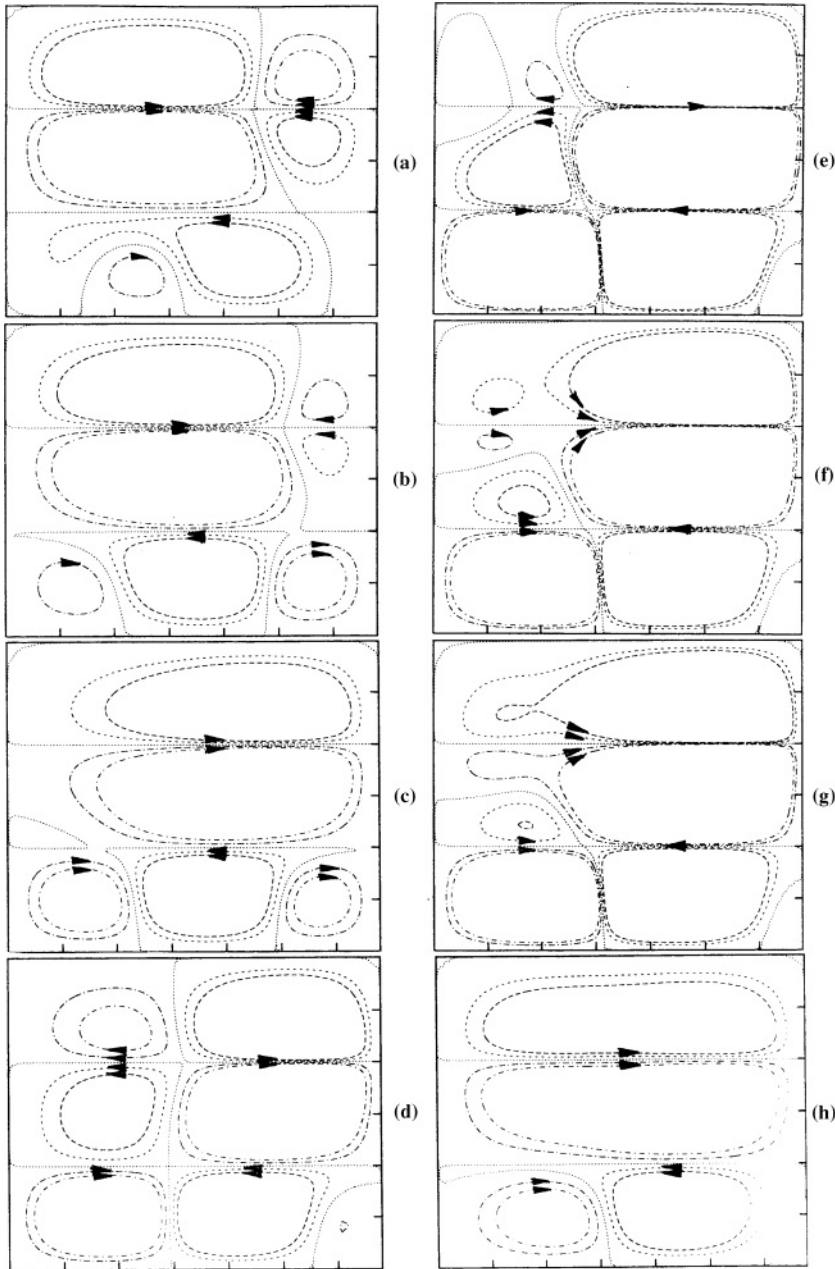


FIG. 8. Snapshots of streamlines for the asymmetric time-periodic motion during one period at $\epsilon = 0.0035$, $G = 2.15$, and $K = 3682$.

where Δx , Δz are the mesh sizes for the corresponding coordinates. Poisson equations were solved by the iterative Liebman successive overrelaxation method at each time step: the accuracy of the solution was 10^{-4} for steady motion and 10^{-5} for oscillations.

The details of the numerical method can be found in the book by Simanovskii and Nepomnyashchy [1] (see also [11]).

IV. NUMERICAL RESULTS

Let us consider the system air–ethylene glycol–fluorinert FC75 with the following set of parameters: $\nu = 0.974$, $\nu_* = 18.767$, $\eta = 0.001$, $\eta_* = 0.013$, $\kappa = 0.098$, $\kappa_* = 0.401$, $\chi = 215.098$, $\chi_* = 606.414$, $\beta = 5.9$, $\beta_* = 2.62$, $P = 0.72$, and $\bar{\alpha} = 0.080$. Fix the ratios of the layer thicknesses $a = a_* = 1$. Nonlinear simulations have been performed for $L = 3.4$. This system was chosen for the following reasons. First, this system

is appropriate for Earth experiments because of the relatively low viscosity of the fluorinert. An extensive experimental investigation of convection in the present system was performed by Prakash and Koster (see [12]). Scientific interest in this system owes to the fact that it is subject to different kinds of instabilities driven by different interfaces. For the system under consideration, the flow of thermocapillary origin takes place mainly near the upper interface. The flow of buoyancy origin develops mainly in the bottom layer. The “indirect” interaction of both mechanisms of instability can lead to much more complex dynamics (in comparison with two-layer systems) and various unexpected effects. Evidently, such an “indirect” interaction is impossible in a system with a single interface.

A. The case $\epsilon = 0$

Under the conditions of the experiment, when the geometric configuration of the system is fixed while the temperature

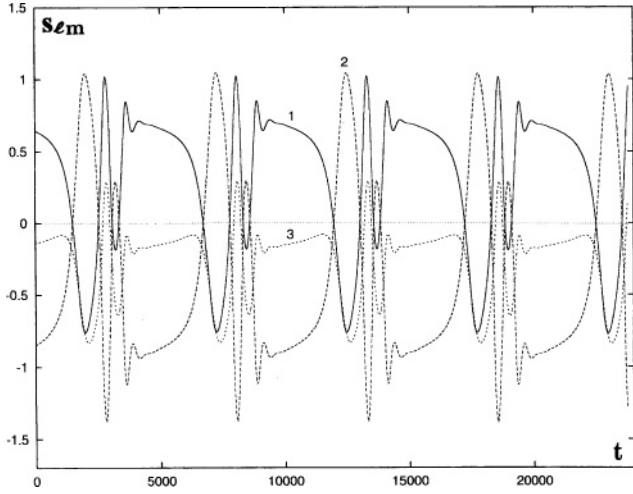


FIG. 9. Dependencies of $S_{l,m}$ on time ($m = 1, 2, 3$) at $\epsilon = 0.0035$, $G = 2.15$, and $K = 3682$.

difference θ is changed, the Marangoni number M and the Grashof number G are proportional. It is convenient to define a parameter that does not change when θ is changed. We define the inverse dynamic Bond number

$$K = \frac{M}{GP} = \frac{\alpha}{g\beta_1\rho_1 a_1^2}.$$

Let us fix $K = 3682$. When the Grashof number is small enough, the system maintains mechanical equilibrium. With an increase in the Grashof number, the mechanical equilibrium state becomes unstable, and perfectly symmetric standing waves (type 1) satisfying symmetry conditions

$$\begin{aligned} \psi_m(L-x, z, t) &= -\psi_m(x, z, t), \\ T_m(L-x, z, t) &= T_m(x, z, t), \quad m = 1, 2, 3, \end{aligned} \quad (29)$$

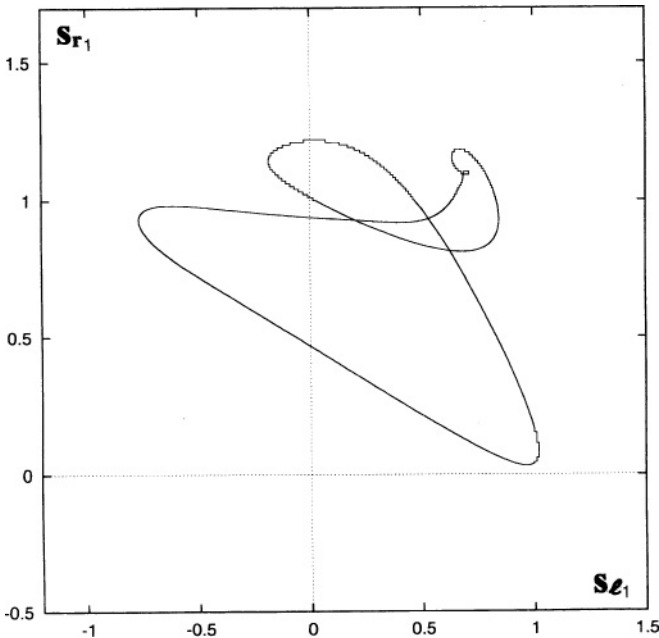


FIG. 10. Phase trajectory in the plane (S_{l1}, S_{r1}) for asymmetric oscillatory motion at $\epsilon = 0.0035$, $G = 2.15$, and $K = 3682$.

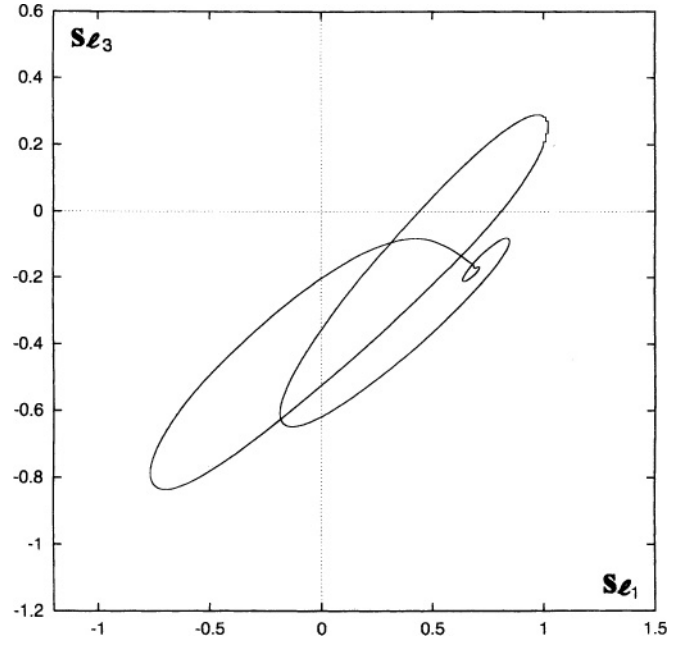


FIG. 11. Phase trajectory in the plane (S_{l1}, S_{l3}) for asymmetric oscillatory motion at $\epsilon = 0.0035$, $G = 2.15$, and $K = 3682$.

develop near the instability threshold (see [13]). Snapshots of streamlines during one period are shown in Fig. 2. One can see that the direction of the vortex rotation in the cavity is changed during half of this period [cf. Figs. 2(a) and 2(d)].

We use the following integral quantities, characterizing the intensity of motions in the left and in the right halves of the layers:

$$S_{l1}(t) = \int_0^{L/2} dx \int_0^1 dz \psi_1(x, z, t), \quad (30)$$

$$S_{r1}(t) = \int_{L/2}^L dx \int_0^1 dz \psi_1(x, z, t);$$

$$S_{l2}(t) = \int_0^{L/2} dx \int_{-a}^0 dz \psi_2(x, z, t), \quad (31)$$

$$S_{r2}(t) = \int_{L/2}^L dx \int_{-a}^0 dz \psi_2(x, z, t);$$

$$S_{l3}(t) = \int_0^{L/2} dx \int_{-a-a_*}^{-a} dz \psi_3(x, z, t), \quad (32)$$

$$S_{r3}(t) = \int_{L/2}^L dx \int_{-a-a_*}^{-a} dz \psi_3(x, z, t).$$

The time evolution of the quantities $S_{lm}(t)$, $m = 1, 2, 3$, for $G = 2.15$, is shown in Fig. 3 (lines 1a, 2a, and 3a). The phase trajectory presented in Fig. 4 (line 1) shows a significant phase delay of oscillations in the top layer with respect to oscillations in the bottom layer.

B. The case $\epsilon \neq 0$

Let us now consider the influence of a horizontal component of the temperature gradient on the structures described above. For any $\epsilon \neq 0$, symmetry conditions (29) are violated and

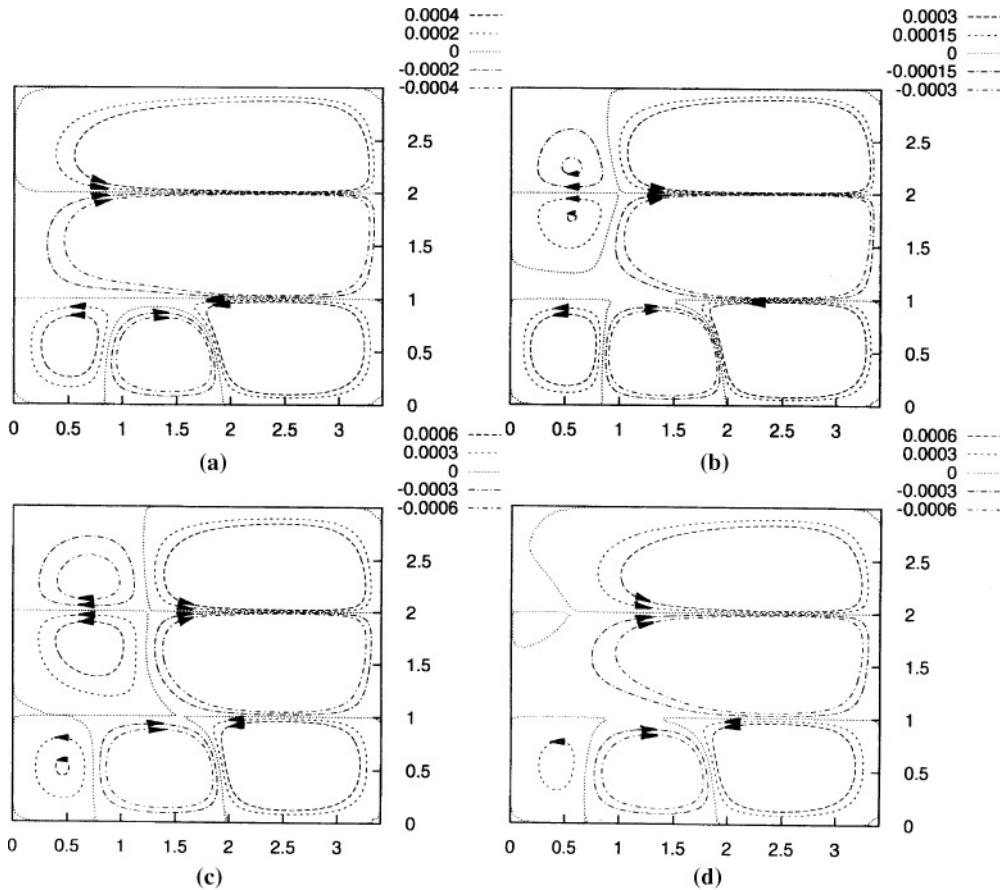


FIG. 12. Snapshots of streamlines for $\epsilon = 0.01$, $G = 2.15$, and $K = 3682$.

asymmetric oscillatory motion takes place in the system. Snapshots of streamlines for this type of motion during the period of oscillations $0 < t < \tau$ are presented in Fig. 5. One can see that, in comparison with the symmetric oscillatory flow shown in Fig. 2, the vortices have the tendency to become longer. The period of asymmetric oscillations changes in a nonmonotonic way (see Fig. 6, line 1). At $\epsilon > 0.000875$,

asymmetric oscillations become unstable and an asymmetric steady flow appears in the system. Streamlines of the steady state are shown in Fig. 7. At $\epsilon > 0.0029$, the asymmetric steady flow is destroyed and an asymmetric oscillatory flow (type 2) is developed in the system. The snapshots of streamlines during one period for $\epsilon = 0.0035$, are shown in Fig. 8. The

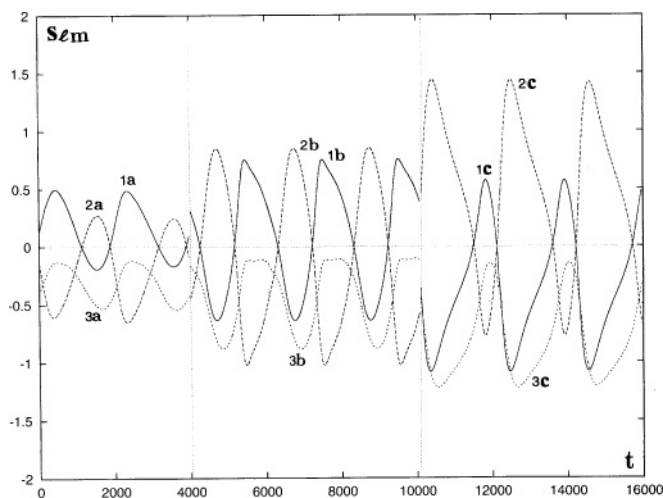


FIG. 13. Dependencies of $S_{l,m}$ on time ($m = 1, 2, 3$) at $G = 2.15$ (lines 1a, 2a, 3a), $G = 2.20$ (lines 1b, 2b, 3b), and $G = 2.365$ (lines 1c, 2c, 3c); $\epsilon = 0.01$, $K = 3682$.

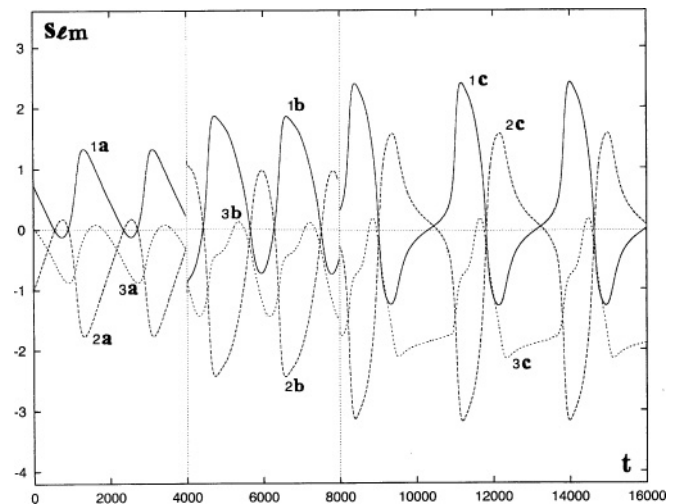


FIG. 14. Dependencies of $S_{l,m}$ on time ($m = 1, 2, 3$) at $G = 2.50$ (lines 1a, 2a, 3a), $G = 2.70$ (lines 1b, 2b, 3b), and $G = 3.30$ (lines 1c, 2c, 3c); $\epsilon = 0.03$, $K = 3682$.

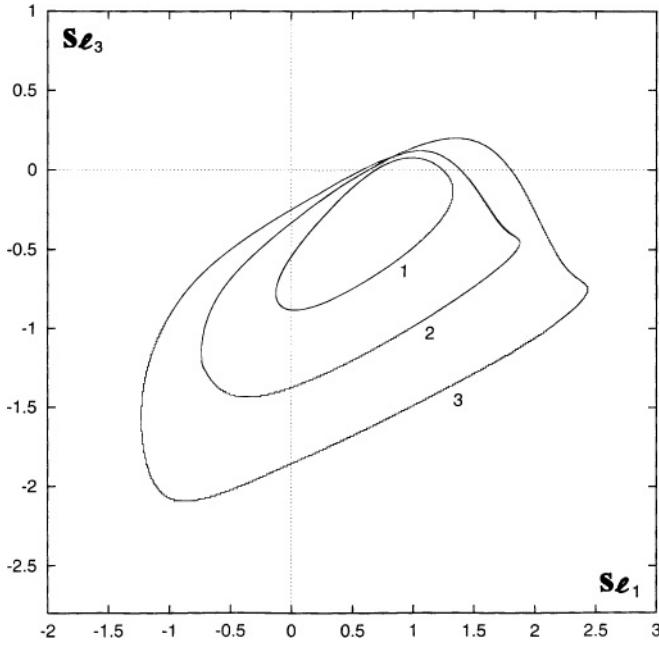


FIG. 15. Phase trajectories in the plane (S_{11}, S_{13}) for $G = 2.50$ (line 1), $G = 2.70$ (line 2), and $G = 3.30$ (line 3); $\epsilon = 0.03$; $K = 3682$.

time evolution of quantities $S_{lm}(t)$, $m = 1, 2, 3$, for asymmetric oscillations is presented in Fig. 9. One can see that oscillations become rather complicated, maintaining the periodic form. The phase trajectories of the asymmetric oscillations in variables (S_{11}, S_{r1}) and (S_{11}, S_{13}) have a multiloop character (see Figs. 10 and 11).

With an increase in ϵ , the period of oscillations decreases (Fig. 6, line 2). The dependencies $S_{lm}(t)$, $m = 1, 2, 3$, for $\epsilon = 0.01$ are presented in Fig. 3 (lines 1b, 2b, and 3b) and the corresponding phase trajectory is shown in Fig. 4 (line 2). With further increase in ϵ at fixed values of G and K , the asymmetric oscillatory flow disappears and a stationary structure with long cells in each fluid layer is preferentially formed in the system.

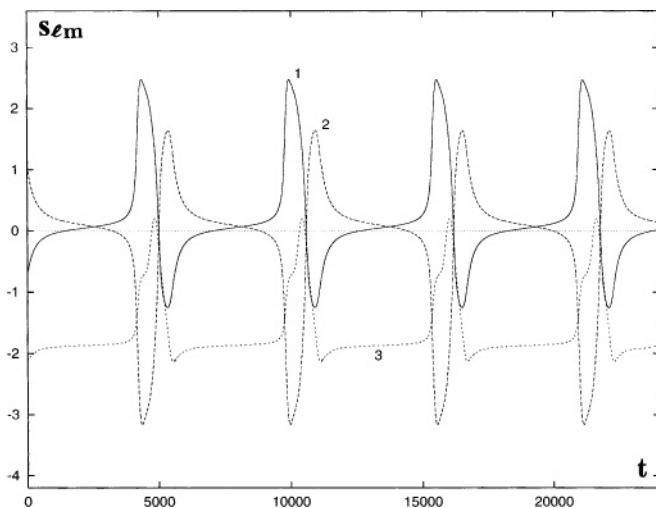


FIG. 16. Dependencies of $S_{l,m}$ on time ($m = 1, 2, 3$) at $\epsilon = 0.03$, $G = 3.35$, and $K = 3682$.

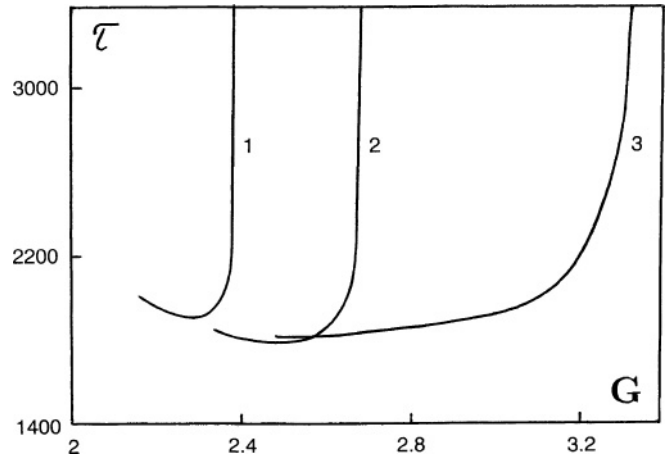


FIG. 17. Dependencies of the period of oscillations on the Grashof number G ; $\epsilon = 0.01$ (line 1); $\epsilon = 0.018$ (line 2), and $\epsilon = 0.03$ (line 3); $K = 3682$.

Now let us increase G at fixed values of ϵ and K . We take $\epsilon = 0.01$. For sufficiently small values of the Grashof number, steady asymmetric flow appears in the system. For $G > 2.085$, the steady state is destroyed and asymmetric oscillations (type 3) develop (see Fig. 12). The dependencies of $S_{lm}(t)$, $m = 1, 2, 3$, for different values of G , are presented in Fig. 13. At $G > 2.374$, the oscillatory flow becomes unstable and an asymmetric steady state occurs in the system. This means that the region of nonlinear asymmetric oscillations is restricted by the Grashof number values, both from below and from above, by the regions of the steady states.

Let us fix $\epsilon = 0.03$. For $G > 2.475$, the asymmetric steady state is destroyed and asymmetric oscillatory flow develops in the system. The dependencies of $S_{lm}(t)$, $m = 1, 2, 3$, for different values of G , are presented in Fig. 14. The corresponding phase trajectories are shown in Fig. 15. With an increase in G , the period of oscillations becomes extremely high (see Fig. 16). One can see a “plateau” for the functions $S_{lm}(t)$ in Fig. 16. This means that the streamlines as well as the temperature fields change slightly over a relatively long time interval. With a further increase in G , the oscillations disappear. For G close to $G_* = 3.35$, the period of oscillations τ satisfies the relation $\tau^{-2} \sim G_* - G$, which is characteristic for a saddle-node bifurcation. When $G > G_*$, the steady asymmetric motion takes place in the system.

The dependencies of the period of oscillations on the Grashof number for different values of ϵ are presented in Fig. 17.

V. CONCLUSION

The influence of the horizontal component of the temperature gradient on nonlinear regimes of oscillatory convection developed under the joint action of buoyant and thermocapillary effects in a multilayer system is investigated. Transitions between different flow regimes have been studied. It is shown that for $\epsilon \neq 0$, asymmetric oscillatory motion takes place in the system. In comparison with the symmetric oscillatory flow, the vortices for the asymmetric oscillations have the tendency to become longer. At a definite interval of ϵ , the phase trajectories

of the asymmetric oscillations have a multiloop character. With an increase in ϵ , the oscillatory flow becomes unstable and a steady asymmetric state develops in the system. It is found that

for $\epsilon \neq 0$, the region of nonlinear asymmetric oscillations is restricted by the Grashof number values, both from below and from above, by the regions of the steady states.

-
- [1] I. B. Simanovskii and A. A. Nepomnyashchy, *Convective Instabilities in Systems with Interface* (Gordon and Breach, London, 1993).
- [2] A. Nepomnyashchy, I. Simanovskii, and J.-C. Legros, *Interfacial Convection in Multilayer Systems* (Springer, New York, 2006).
- [3] G. Z. Gershuni and E. M. Zhukhovitsky, *Convective Stability of Incompressible Fluid* (Keter, Jerusalem, 1976).
- [4] J. R. A. Pearson, *J. Fluid Mech.* **4**, 489 (1958).
- [5] A. A. Nepomnyashchy and I. B. Simanovskii, *Fluid Dyn.* **19**, 494 (1984).
- [6] A. Juel, J. M. Burgess, W. D. McCormick, J. B. Swift, and H. L. Swinney, *Physica D* **143**, 169 (2000).
- [7] A. A. Nepomnyashchy, I. B. Simanovskii, and L. M. Braverman, *Phys. Fluids* **17**, 022103 (2005).
- [8] I. B. Simanovskii, A. Viviani, F. Dubois, and J.-C. Legros, *C.R. Mecanique* **337**, 75 (2009).
- [9] I. B. Simanovskii, *Phys. Rev. E* **79**, 056313 (2009).
- [10] I. Simanovskii, A. Nepomnyashchy, V. Shevtsova, P. Colinet, and J. C. Legros, *Phys. Rev. E* **73**, 066310 (2006).
- [11] A. A. Nepomnyashchy and I. B. Simanovskii, *Phys. Rev. E* **59**, 6672 (1999).
- [12] A. Prakash and J. N. Koster, *Eur. J. Mech. B Fluids* **12**, 635 (1993).
- [13] I. B. Simanovskii, A. Viviani, F. Dubois, and J.-C. Legros, *Phys. Fluids* **23**, 012103 (2011).